Available online at www.sciencedirect.com
ScienceDirect
Carbohydrate Research 343 (2008) 1237–1250
Carbohydrate RESEARCH

Structural analysis of the α-D-glucan (EPS180) produced by the *Lactobacillus reuteri* strain 180 glucansucrase GTF180 enzyme

Sander S. van Leeuwen,[a] Slavko Kralj,[b,c] Ineke H. van Geel-Schutten,[c,†] Gerrit J. Gerwig,[a] Lubbert Dijkhuizen[b,c] and Johannis P. Kamerling[a,*]

[a]*Bijvoet Center, Department of Bio-Organic Chemistry, Utrecht University, Padualaan 8, 3584 CH Utrecht, The Netherlands*
[b]*Department of Microbiology, Groningen Biomolecular Sciences and Biotechnology Institute, University of Groningen, Kerklaan 30, 9751 NN Haren, The Netherlands*
[c]*Centre for Carbohydrate Bioprocessing, TNO—University of Groningen, Kerklaan 30, 9751 NN Haren, The Netherlands*

Received 2 November 2007; received in revised form 15 January 2008; accepted 30 January 2008
Available online 7 February 2008

Abstract—The neutral exopolysaccharide **EPS180** produced from sucrose by the glucansucrase GTF180 enzyme from *Lactobacillus reuteri* 180 was found to be a (1→3,1→6)-α-D-glucan, with no repeating units present. Based on linkage analysis, periodate oxidation, and 1D/2D ^{1}H and ^{13}C NMR spectroscopy of the intact **EPS180**, as well as MS and NMR analysis of oligosaccharides obtained by partial acid hydrolysis of **EPS180**, a composite model, that includes all identified structural features, was formulated as follows:

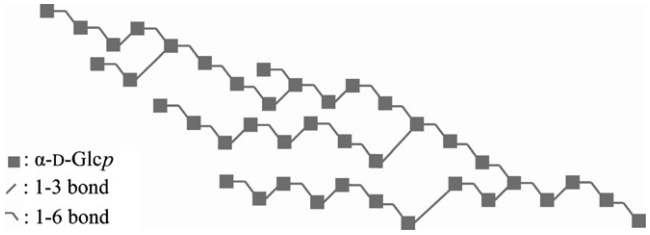

Keywords: α-D-Glucan; Polysaccharide structural analysis; GTF180 Glucansucrase; ^{1}H NMR spectroscopy; *Lactobacillus reuteri* 180

1. Introduction

Lactic acid bacteria (LAB), like *Lactobacilli*, produce exopolysaccharides (EPSs) that are excreted into their surroundings. The complex functions of the EPSs in vivo are not fully understood but seem to be mostly of a protective nature. Exopolysaccharides have been shown to be involved in adhesion,[1] certain cellular recognition processes,[2] and protection against dehydration, phagocytosis or toxins.[2] It is unlikely that these EPSs are being produced as a food reserve, as most LAB do not have the enzymes to catabolise these EPSs.[3] Because of their physical properties that lie at the basis of their protective nature, the food and dairy industry is interested in these exopolysaccharides as thickeners, stabilisers and gelling agents.[4]

So far, most structurally characterised exopolysaccharides from LAB are heteropolysaccharides with repeating-unit structures.[5] Structures of LAB homopolysaccharides produced by specific glucansucrase enzymes have not been extensively investigated. Only

* Corresponding author. Tel.: +31 30 253 3479; fax: +31 30 254 0980; e-mail: j.p.kamerling@uu.nl
† Present address: Materials Innovation Centre B.V., Julianalaan 136, 2628 BL Delft, The Netherlands.

0008-6215/$ - see front matter © 2008 Elsevier Ltd. All rights reserved.
doi:10.1016/j.carres.2008.01.042

initial structural studies have been performed on dextrans (polysaccharides containing mostly (α1→6) linkages) with (α1→2), (α1→3) and (α1→4) branches,[6,7] or linear homopolysaccharides.[8]

Recently, a family of glucansucrases was discovered in *Lactobacillus reuteri*, which converts sucrose into large, heavily branched α-glucans. One of these glucansucrases (GTF180) produces **EPS180**, an α-glucan with (α1→3) and (α1→6) glycosidic linkages.[9] The GTF180 enzyme shows large similarity with other glucansucrase enzymes, but has a relatively large N-terminal variable region. Truncation of the enzyme, by deletion of the variable region, had no effect on the linkage distribution of the α-glucan produced.[9] The unique polysaccharide structure produced was suggested to be pre-biotic.[10] Here, we describe the structural analysis of this homopolysaccharide, leading to the formulation of a composite model that includes the various structural features established.

2. Results

2.1. Composition of EPS180

Monosaccharide analysis of **EPS180** revealed the presence of glucose only, and a carbohydrate content of 100% (w/w). Methylation analysis of **EPS180** showed the presence of terminal, 3-substituted, 6-substituted and 3,6-disubstituted glucopyranose in a molar percentage of 12%, 24%, 52% and 12%. 1D ^{1}H NMR spectroscopy (Fig. 1A) indicated an α-anomeric configuration for all glucose residues. Of these residues, 69% is involved in (α1→6) linkages ($\delta_{H\text{-}1} \sim 4.96$) and 31% in

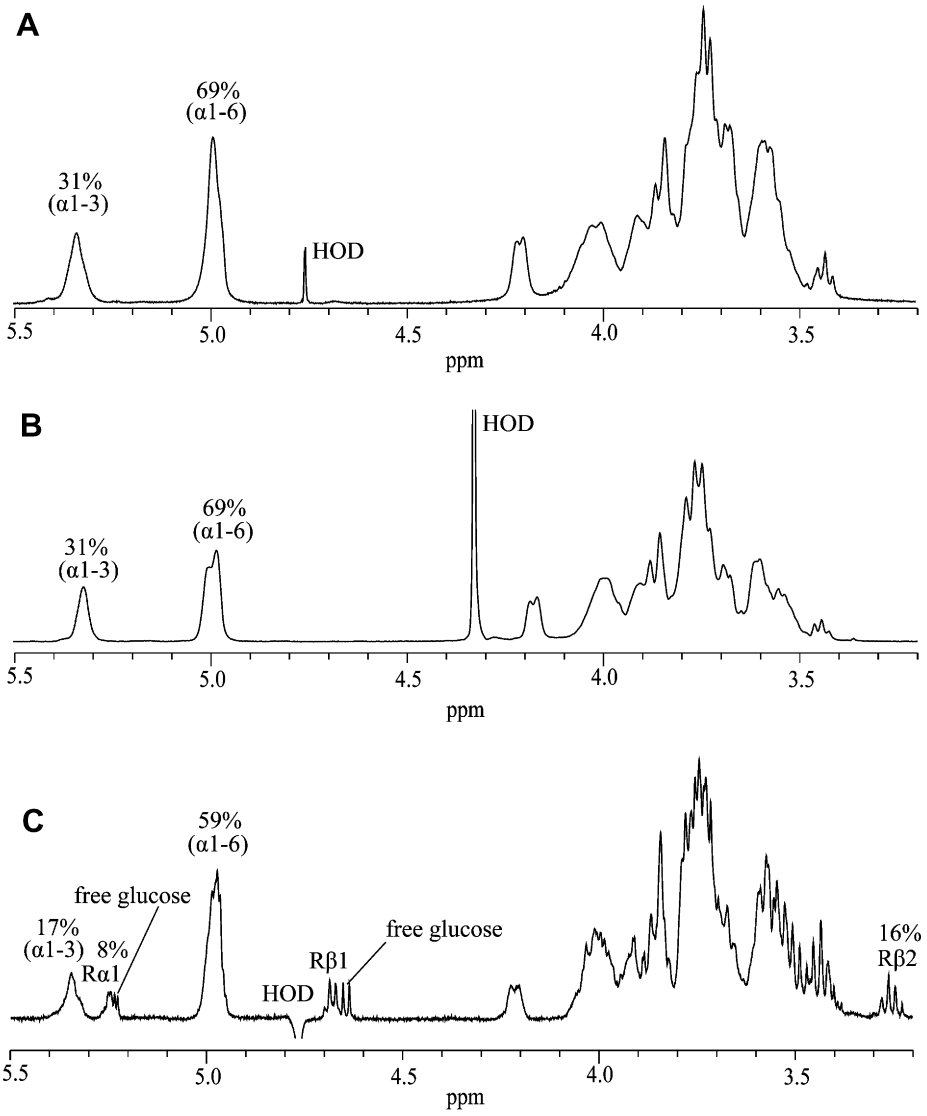

Figure 1. 500-MHz 1D ^{1}H NMR spectra of (A) intact **EPS180** recorded at 300 K in D_2O; (B) intact **EPS180** recorded at 330 K in D_2O; and (C) **EPS180** partial acid hydrolysate recorded at 300 K in D_2O.

(α1→3) linkages ($\delta_{H\text{-}1}$ 5.33), which is in agreement with the linkage distribution found by methylation analysis (see also Ref. 9). In the 1D ^{1}H NMR spectrum recorded at 330 K (Fig. 1B), the (α1→6) anomeric signal is split into two overlapping peaks, while the (α1→3) anomeric signal remains a single peak. This may suggest that the (-)α-D-Glc*p*-(1→3)-[‡] residues in **EPS180** are present in a uniform structural element. The splitting of the (α1→6) anomeric ^{1}H signal in the spectrum recorded at 330 K indicates at least two specific structural elements for (-)α-D-Glc*p*-(1→6)- residues.

2.2. Partial acid hydrolysis

After having evaluated different acid hydrolysis conditions, making use of MALDI-TOF-MS and ^{1}H NMR analyses, a large batch of **EPS180** (500 mg) was subjected to partial acid hydrolysis, using 0.5 M TFA (3 h, 90 °C). The latter conditions generated a pool of oligosaccharides with different degrees of polymerisation, as evidenced by ^{1}H NMR spectroscopy (Fig. 1C) and HPAEC on CarboPac PA-100 (Fig. 2A). The 1D ^{1}H NMR spectrum of the pool (Fig. 1C) showed a strong reduction of the anomeric signal corresponding to (α1→3)-linked Glc residues, while the relative amount of (α1→6)-linked Glc residues was only slightly reduced, indicating that the (α1→3) linkages are more susceptible to acid hydrolysis with TFA than the (α1→6) linkages. Moreover, the surface area of the H-4 signal at δ 3.40–3.45, previously identified as a structural-reporter-group signal for non-reducing terminal α-D-Glc*p* residues,[11] corresponds with the collective surface area of the reducing α- and β-D-Glc*p* H-1 signals, indicating a particular lability around branch points. The glycan pool was pre-fractionated on Bio-Gel P-4, and three subpools were isolated, denoted **I**–**III**. The fragment size distribution within each subpool was determined by MALDI-TOF-MS (data not shown). Subpool **I** contained fragments in a size range up to seven Glc units, subpool **II** fragments from five up to nine glucose units and subpool **III** from seven Glc units and larger. As subpool **III** consisted mainly of oligosaccharides too large for full structural analysis, it was not further studied. Subpools **I** and **II** were subfractionated by HPAEC on CarboPac PA-1, using a 0–300 mM NaOAc gradient in 100 mM NaOH (Fig. 2B), and fractions **1** to **6** were isolated from subpool **I**, and **7** and **8** from subpool **II**.

[‡] For Glc residues at semi-defined places in the structure (-)α-D-Glc*p*-(1→*x*)- or -(1→*x*)-α-D-Glc*p*(-) is used. When the structural context of the residue is precisely known, this is indicated as follows: -(1→*x*)-α-D-Glc*p*-(1→*y*)- describing an *x*-substituted residue with an (1→*y*) linkage. In case of a non-reducing terminal residue α-D-Glc*p*-(1→*x*)- is used, a reducing terminal residue is indicated with -(1→*x*)-D-Glc*p*.

2.2.1. Fraction 1. ^{1}H NMR analysis of fraction **1** revealed the presence of only one compound that corresponds with isomaltotriose, α-D-Glc*p*-(1→6)-α-D-Glc*p*-(1→6)-D-Glc*p* (Scheme 1).[11]

2.2.2. Fraction 2. MALDI-TOF-MS analysis of fraction **2** showed an $[M+Na]^+$ pseudomolecular ion at *m*/*z* 689, corresponding with Hex_4. The ^{1}H NMR spectrum showed a multiple anomeric signal, corresponding to three protons, at $\delta \sim 4.96$, reflecting the presence of α-D-Glc*p*-(1→6)- (residue **D**) and -α-D-Glc*p*-(1→6)- (residue **C**) units.[11] Furthermore, the H-1α and H-1β resonances of the reducing unit **R** (δ 5.240 and 4.669) are in agreement with a -(1→6)-D-Glc*p* unit.[11] Therefore, fraction **2** contains isomaltotetraose, α-D-Glc*p*-(1→6)-α-D-Glc*p*-(1→6)-α-D-Glc*p*-(1→6)-D-Glc*p* (Scheme 1).

2.2.3. Fraction 3. The MALDI-TOF mass spectrum of fraction **3** revealed $[M+Na]^+$ pseudomolecular ions at *m*/*z* 689 and 851, corresponding with Hex_4 and Hex_5, respectively. Fraction **3** was further separated by HPAEC on CarboPac PA-1, isocratically eluted with 100 mM NaOAc in 100 mM NaOH (Fig. 2C), yielding two fractions denoted **3a** and **3b**.

The MALDI-TOF mass spectrum of fraction **3a** showed one peak at *m*/*z* 851, corresponding to the $[M+Na]^+$ pseudomolecular ion of Hex_5. The ^{1}H NMR spectrum (not shown) revealed one multiple anomeric signal at $\delta \sim 4.96$ (4H) and two anomeric signals corresponding to the reducing residue **R** at δ 5.241 and 4.671. On guidance of the earlier developed structural-reporter-group concept,[11] the signal at $\delta \sim 4.96$ indicates the presence of α-D-Glc*p*-(1→6)- (residue **D**) and -α-D-Glc*p*-(1→6)- (residues **C**) units. The chemical shift positions of H-1α and H-1β of the reducing residue **R** are in agreement with the occurrence of a -(1→6)-D-Glc*p* unit. Considering all analytical data, fraction **3a** is identified as isomaltopentaose, α-D-Glc*p*-(1→6)-α-D-Glc*p*-(1→6)-α-D-Glc*p*-(1→6)-α-D-Glc*p*-(1→6)-D-Glc*p* (Scheme 1).

MALDI-TOF-MS analysis of fraction **3b** gave rise to one $[M+Na]^+$ pseudomolecular ion at *m*/*z* 689, corresponding with Hex_4. The 1D ^{1}H NMR spectrum (Fig. 3) showed five anomeric signals at δ 5.345/5.336 (**B** H-1, $^3J_{1,2}$ 3.8 Hz), 5.249 (**Rα** H-1, $^3J_{1,2}$ 3.8 Hz), 4.965 (**D** H-1, $^3J_{1,2}$ 3.8 Hz), 4.958 (**A** H-1, $^3J_{1,2}$ 3.8 Hz) and 4.680 (**Rβ** H-1, $^3J_{1,2}$ 7.6 Hz). The splitting of the **B** H-1 signal into two doublets is due to the influence of the α/β configuration of the reducing residue **R**. Note that the intensity of the **Rβ** H-1 signal is influenced by the pre-saturation of the HOD signal. Therefore, in quantifications the surface area of **Rβ** H-2 ($\delta \sim 3.27$) is used. Starting from the anomeric signals in the 2D ^{1}H–^{1}H TOCSY spectrum (Fig. 3/180 ms), all chemical shifts of the non-anomeric protons could be determined (Table 1). The **Rα** and **Rβ** H-1 values fit best with those

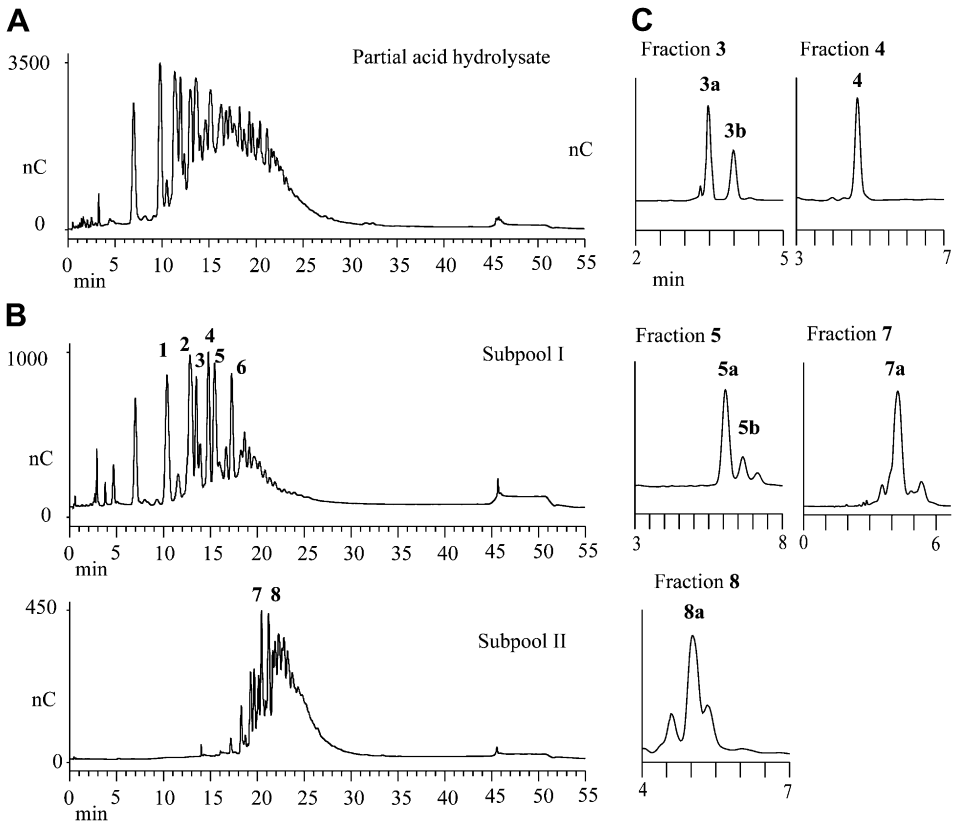

Figure 2. (A) HPAEC profile of **EPS180** partial acid hydrolysate on CarboPac PA-100; (B) HPAEC profiles of Bio-Gel P-4 subpool **I** and subpool **II** on CarboPac PA-1, using a linear gradient; and (C) HPAEC profiles of HPAEC fractions **3**, **4**, **5**, **7** and **8** on CarboPac PA-1, using isocratic conditions. For experimental details, see Section 4.

of a -(1→6)-D-Glc*p* unit (H1α, δ 5.239–5.241; H1β, δ 4.671–4.672),[11] which is further supported by the chemical shifts of **Rα** and **Rβ** H-5 at δ 4.00 and 3.63, respectively (library data: δ 4.01 and 3.64–3.65);[11] compare also the H-6a and H-6b values with library data.[11] Although the anomeric signals of **A** and **D** strongly overlap, the difference in H-2, H-3 and H-4 between the two residues can clearly be observed in the built-up series of mixing times (data not shown). The chemical shifts of the set of **A** H-2, H-3 and H-4 at δ 3.64, 3.85 and 3.67, respectively, correspond with those of a -(1→3)-α-D-Glc*p*(-) unit. The presence of **D** H-4 at δ 3.42 (dd, 1H) reflects the occurrence of one terminal α-D-Glc*p*-(1→*x*)- unit, most probably α-D-Glc*p*-(1→6)- instead of α-D-Glc*p*-(1→3)-,[11] indicating a linear structure; note that the H-4 signals of residues **A** and **B** do not resonate at this value. Taking into account that **R** is -(1→6)-D-Glc*p* (see above), the significant downfield shift of **B** H-5 (δ 4.20) is indicative for an internal -α-D-Glc*p*-**B**-(1→3)-α-D-Glc*p*- element.[11] It should be noted that the downfield shift of **B** H-5 is caused by the occurrence of a hydrogen bond between **B** O-5 and H(O)-2 of the neighbouring Glc residue.[12] When compared with the chemical shift of H-5 of the internal Glc residue in nigerotriose (δ 4.01),[11] a further downfield shift is seen for H-5, which is in favour of a -(1→6)-α-D-Glc*p*-**B**-(1→3)- instead of a -(1→3)-α-D-Glc*p*-**B**-(1→3)- element. As residue **D** occurs in terminal position, the **B** H-5 signal indicates a **B**1→3**A** sequence, which means that the total sequence has to be **D**1→6**B**1→3**A**1→6**R**, that is, α-D-Glc*p*-(1→6)-α-D-Glc*p*-(1→3)-α-D-Glc*p*-(1→6)-D-Glc*p* (Scheme 1).

The established structure of the tetrasaccharide was verified by 2D ^{13}C–^{1}H HSQC and ROESY measurements. Interpretation of the HSQC spectrum (Fig. 3) yielded $\delta_{C\text{-}6}$ values of 66.5 ppm for both residue **R** and **B**, and 61.2 ppm for residues **A** and **D**, indicating 6-substituted **R** and **B** units.[13] The $\delta_{C\text{-}3}$ value of 81.2 ppm of residue **A** indicated a 3-substituted **A** unit.[13] In the ROESY spectrum (Fig. 3), inter-residual cross-peaks were observed between **A** H-1 and **R** H-6a, between **B** H-1 and **A** H-3 and between **D** H-1 and **B** H-6a.

2.2.4. Fraction 4. MALDI-TOF-MS analysis of fraction **4** showed an $[M+Na]^+$ pseudomolecular ion at *m/z* 851, corresponding with Hex_5. HPAEC analysis on CarboPac PA-1 (eluent: 100 mM NaOAc in 100 mM NaOH) showed only one peak (Fig. 2C). The 1D ^{1}H NMR spectrum (Fig. 4A) revealed six anomeric signals at δ 5.334 (**B** H-1, $^{3}J_{1,2}$ 3.6 Hz), 5.241 (**Rα** H-1, $^{3}J_{1,2}$

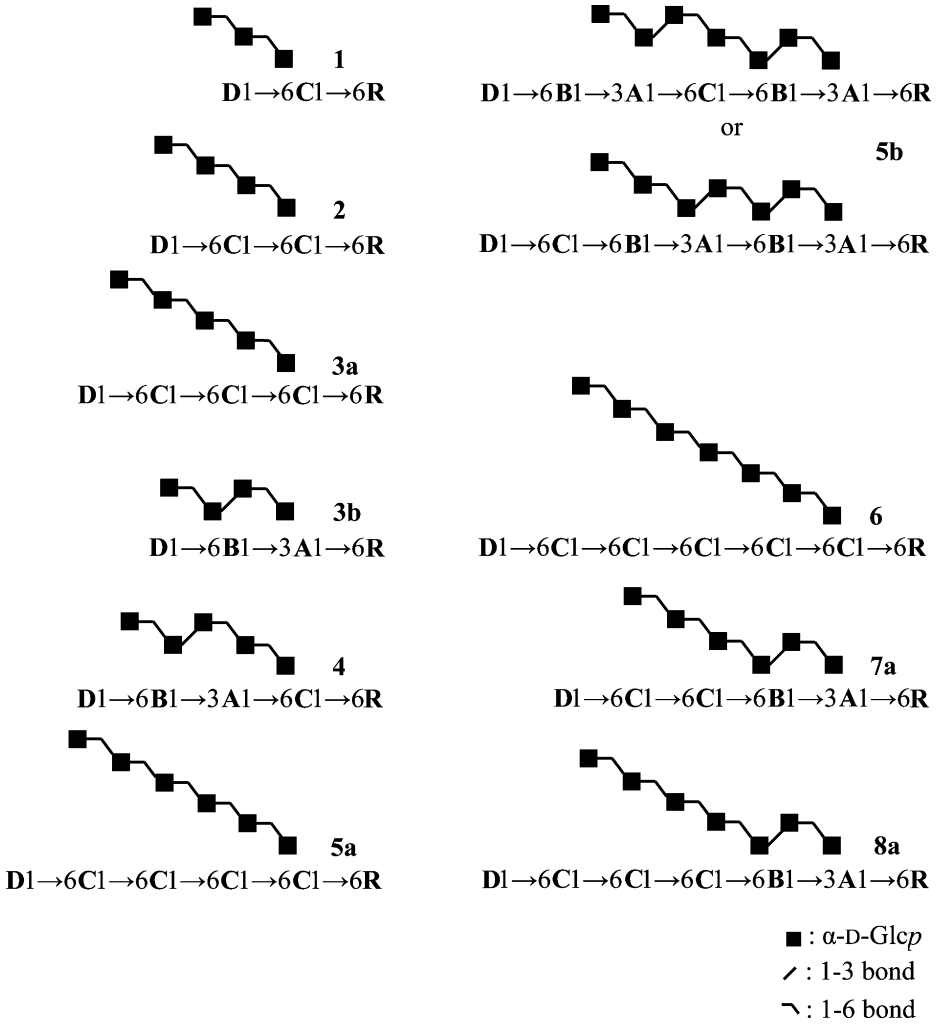

Scheme 1. Structures of oligosaccharide fragments obtained by partial acid hydrolysis of **EPS180**.

3.6 Hz), 4.982 (**A** H-1, $^{3}J_{1,2}$ 3.6 Hz), 4.982 (**C** H-1, $^{3}J_{1,2}$ 3.6 Hz), 4.963 (**D** H-1, $^{3}J_{1,2}$ 3.6 Hz) and 4.670 (**Rβ** H-1, $^{3}J_{1,2}$ 8.0 Hz).

Starting from the anomeric signals in the 2D ^{1}H–^{1}H TOCSY spectrum (not shown), the chemical shifts of all non-anomeric signals could be determined (Table 1). The H-1α and H-1β chemical shifts of the reducing residue **R** correspond to the values established for a -(1→6)-D-Glc*p* unit.[11] The 6-substitution of residue **R** is also reflected in the chemical shift of H-5 at δ 4.00 and 3.63 for the α- and β-configuration, respectively.[11] Note also the positions of H-6a and H-6b, corresponding to the occurrence of a -(1→6)-D-Glc*p* unit. Although the anomeric signals of **A** and **C** overlap, the H-2, H-3 and H-4 signals could be assigned by evaluating the built-up series in TOCSY experiments with incremental mixing times (not shown). The chemical shifts of the set of **A** H-2, H-3 and H-4 are δ 3.65, 3.84 and 3.67, respectively, corresponding with the values of a -(1→3)-α-D-Glc*p*(-) unit.[11] The anomeric proton of residue **A** has a chemical shift in the range established for (-)α-D-Glc*p*-(1→6)- units in the structural-reporter-group concept (library data: δ 4.94–4.96[11]), indicating the occurrence of a -(1→3)-α-D-Glc*p*-(1→6)- unit. The chemical shifts of the set of **C** H-2, H-3 and H-4 at δ 3.58, 3.76 and 3.51, combined with the H-1 signal at δ 4.982 (α1→6), indicate the occurrence of a -(1→6)-α-D-Glc*p*-(1→6)-unit.[11] This is further confirmed by the **C** H-5 chemical shift at δ 3.93, which corresponds to the $\delta_{H\text{-}5}$ of a 6-substituted residue.

The chemical shift of residue **B** H-5 at δ 4.20 was shown to indicate the occurrence of a -(1→6)-α-D-Glc*p*-(1→3)- unit (see compound **3b**). Residue **D** has a well-separated anomeric peak at δ 4.963, reflecting an (-)α-D-Glc*p*-(1→6)- unit. Guided by the structural-reporter-group concept established,[11] **D** H-4 at δ 3.42 indicates a terminal unit. The other chemical shift values of residue **D** also correspond to those expected for a terminal α-D-Glc*p*-(1→6)- unit.[11]

Since residue **A** is a -(1→3)-α-D-Glc*p*-(1→6)- unit and residue **B** was shown to be a -(1→6)-α-D-Glc*p*-(1→3)-unit, it can be concluded that compound **4** has a

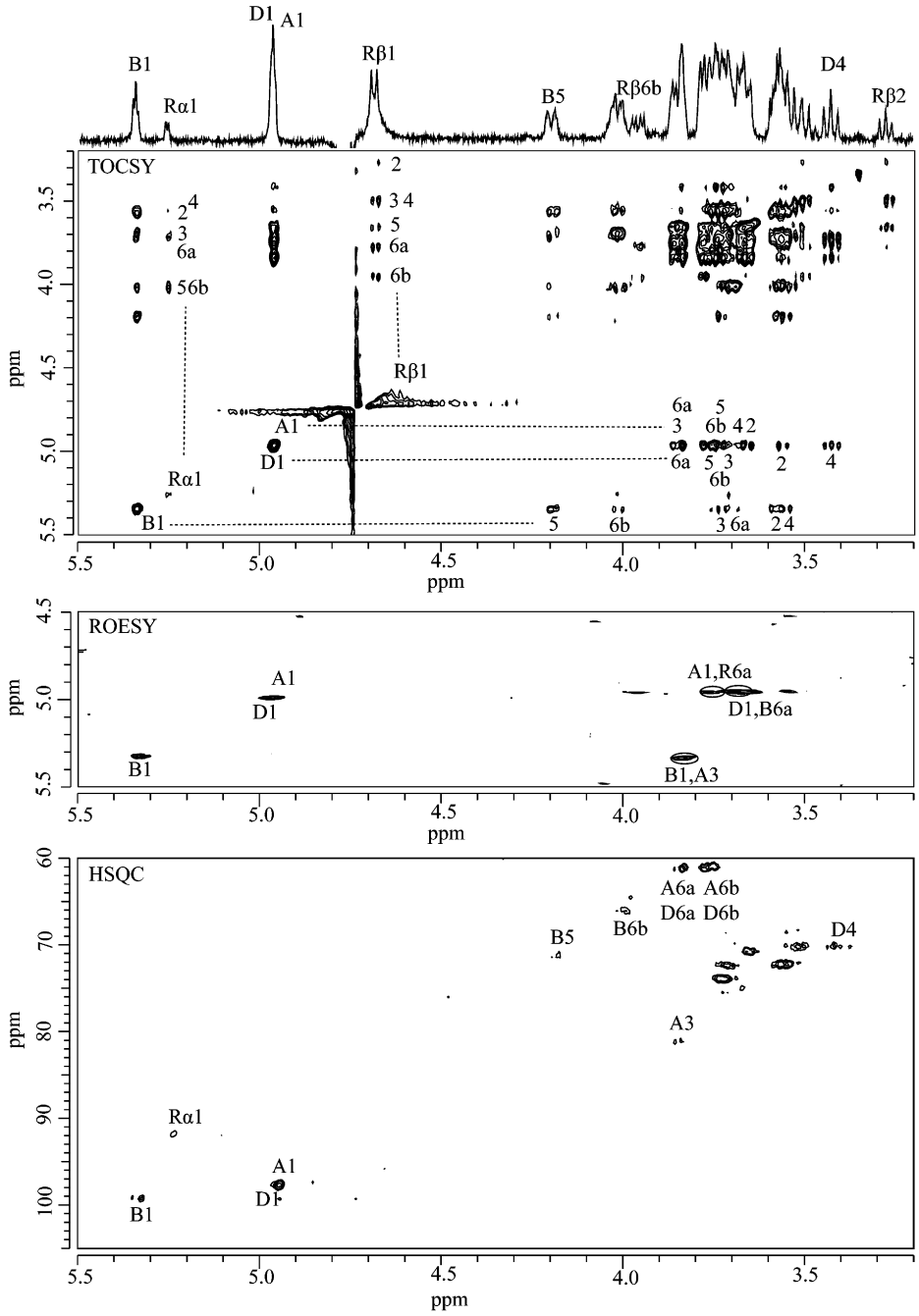

Figure 3. 500-MHz 1D ^{1}H NMR spectrum, 2D ^{1}H–^{1}H TOCSY spectrum (mixing time 180 ms), 2D ^{1}H–^{1}H ROESY spectrum (mixing time 300 ms), and 2D ^{13}C–^{1}H HSQC spectrum of fraction **3b**, recorded at 300 K in D_2O. Anomeric protons in the TOCSY spectrum (Rα1, etc.) have been indicated on the diagonal; numbers in the horizontal and vertical tracks belong to the cross-peaks of the scalar-coupling network of the residues indicated. In the ROESY spectrum, inter-residual couplings (A1,R6a means a cross-peak between **A** H-1 and **R** H-6a, etc.) have been indicated with circles. In the ^{13}C–^{1}H HSQC spectrum, A1 denotes the cross-peak between H-1 and C-1 of residue **A**, etc.

-(1→6)-α-D-Glc*p*-(1→3)-α-D-Glc*p*-(1→6)- element, that is, **X**1→6**B**1→3**A**1→6**Y**. The position of residues **R** and **D** in the structure as reducing and non-reducing termini, respectively, are clear; however, the position of residue **C** cannot be determined from the chemical shift pattern. To assign the position of residue **C** (**D**1→6**B**1→3**A**1→6**C**1→6**R** or **D**1→6**C**1→6**B**1→3**A**1→6**R**), the inter-residual cross-peaks in the ROESY spectrum (not shown) were evaluated. Taking into account the conclusions so far, the shared H-1 track of **A** and **C** showed inter-residual cross-peaks between H-1 and H-6a at δ 3.76–3.77, corresponding with **R** and **C** H-6a. Since residue **C** cannot substitute residue **C**, it can only be residue **A** H-1 interacting with **C** H-6a,

Table 1. ^{1}H chemical shifts of D-glucopyranose residues of oligosaccharide fragments obtained by partial acid hydrolysis of **EPS180** and of intact **EPS180**

Residue	**3b**	**4**	**7a**	**8a**	**EPS180**
Rα-1	5.249	5.241	5.249	5.246	—
Rα-2	3.55	3.55	3.56	3.56	—
Rα-3	3.74	3.74	3.75	3.76	—
Rα-4	3.50	3.50	3.51	3.52	—
Rα-5	4.00	4.00	4.01	3.99	—
Rα-6a	3.74	3.76	3.77	3.77	—
Rα-6b	4.01	4.01	4.00	4.01	—
Rβ-1	4.680	4.670	4.679	4.676	—
Rβ-2	3.26	3.27	3.26	3.27	—
Rβ-3	3.48	3.48	3.48	3.49	—
Rβ-4	3.52	3.52	3.51	3.52	—
Rβ-5	3.63	3.63	3.64	3.63	—
Rβ-6a	3.78	3.75	3.75	3.76	—
Rβ-6b	3.98	3.97	3.98	3.97	—
A-1	4.958	4.982	4.993	4.990	4.99
A-2	3.64	3.65	3.64	3.64	3.65
A-3	3.85	3.84	3.85	3.85	3.87
A-4	3.67	3.67	3.66	3.67	3.66
A-5	3.72	3.73	3.74	3.72	3.70
A-6a	3.85	3.85	3.85	3.84	3.86
A-6b	3.76	3.75	3.75	3.76	3.75
B-1	5.345/5.336	5.334	5.343/5.319	5.343/5.320	5.32
B-2	3.58	3.58	3.59	3.58	3.59
B-3	3.75	3.75	3.74	3.75	3.75
B-4	3.50	3.50	3.50	3.51	3.52
B-5	4.20	4.20	4.21	4.20	4.17
B-6a	3.70	3.71	3.70	3.70	3.72
B-6b	4.01	4.00	4.01	4.01	4.00
C-1	—	4.982	4.972/4.993	4.990/4.968	4.96
C-2	—	3.58	3.58	3.59	3.57
C-3	—	3.76	3.77	3.76	3.76
C-4	—	3.51	3.50	3.51	3.51
C-5	—	3.93	3.94	3.93	3.89
C-6a	—	3.77	3.77	3.77	3.76
C-6b	—	3.99	3.98	3.98	3.95
D-1	4.965	4.963	4.972	4.968	4.96
D-2	3.56	3.55	3.55	3.54	3.55
D-3	3.75	3.75	3.75	3.76	3.76
D-4	3.42	3.42	3.43	3.43	3.41
D-5	3.77	3.77	3.78	3.78	3.78
D-6a	3.85	3.85	3.85	3.85	3.86
D-6b	3.76	3.76	3.75	3.76	3.77
E-1	—	—	—	—	4.99
E-2	—	—	—	—	3.65
E-3	—	—	—	—	3.86
E-4	—	—	—	—	3.77
E-5	—	—	—	—	3.90
E-6a	—	—	—	—	3.75
E-6b	—	—	—	—	3.95

Residue labels correspond to those used in Scheme 1.

and **C** H-1 with **R** H-6a. This finding is confirmed by the presence of the **D** H-1, **B** H-6a (δ 3.71) cross-peak (absence of **D** H-1, **C** H-6a cross-peak), leading unequivocally to **D**1→6**B**1→3**A**1→6**C**1→6**R**, that is, α-D-Glc*p*-(1→6)-α-D-Glc*p*-(1→3)-α-D-Glc*p*-(1→6)-α-D-Glc*p*-(1→6)-D-Glc*p* (Scheme 1).

The substitution pattern of the established structure of compound **4** was verified by 2D ^{13}C–^{1}H HSQC spectroscopy. In the HSQC spectrum (not shown), the $\delta_{C\text{-}6}$ value of 66.8 ppm reflects the 6-substitution of residues **B**, **C** and **R**, in contrast to the $\delta_{C\text{-}6}$ value of 61.3 ppm for residues **A** and **D**.[13] The 3-substitution of residue **A** is evident from the $\delta_{C\text{-}3}$ value of 81.3 ppm.[13]

2.2.5. Fraction 5. Analysis by MALDI-TOF-MS revealed two $[M+Na]^{+}$ pseudomolecular ions with *m*/*z* 1013 and 1175, corresponding with Hex_6 and Hex_7, respectively. Fraction **5** was further separated on CarboPac PA-1 (eluent: 100 mM NaOAc in 100 mM NaOH), yielding a major fraction **5a** and a minor fraction **5b** (Fig. 2C).

The MALDI-TOF mass spectrum of fraction **5a** showed an $[M+Na]^{+}$ pseudomolecular ion at *m*/*z* 1013, in accordance with Hex_6. The ^{1}H NMR spectrum of fraction **5a** (not shown) showed a multiple anomeric signal at $\delta \sim 4.96$ (5H), indicating five (-)α-D-Glc*p*-(1→6)- units.[11] The H-1α and H-1β values of the reducing residue **R** at δ 5.241 and 4.671, respectively, indicate the occurrence of a -(1→6)-D-Glc*p* residue. On guidance of the structural-reporter-group concept,[11] the signal at δ 3.42 (dd, 1H) was identified as H-4 of a α-D-Glc*p*-(1→*x*)- residue, in this case an α-D-Glc*p*-(1→6)- unit. The combined data identified compound **5a** as isomaltohexaose, that is, α-D-Glc*p*-(1→6)-α-D-Glc*p*-(1→6)-α-D-Glc*p*-(1→6)-α-D-Glc*p*-(1→6)-α-D-Glc*p*-(1→6)-D-Glc*p* (Scheme 1).

The MALDI-TOF-MS analysis of fraction **5b** revealed an $[M+Na]^{+}$ pseudomolecular ion at *m*/*z* 1175, corresponding with Hex_7. The sample contained insufficient material for full 2D NMR spectroscopic analysis. The 1D ^{1}H NMR spectrum (Fig. 4B) showed anomeric peaks at δ 5.334 (residues **B**, 2H; (-)α-D-Glc*p*-(1→3)-), 5.248 (residue **Rα**), ~4.96 (residues **A**, **C** and **D**, 4H; (-)α-D-Glc*p*-(1→6)-), and 4.678 (residue **Rβ**). The H-1α and H-1β values of residue **R** correspond best with the occurrence of a -(1→6)-D-Glc*p* residue, and resemble the values found for **3b**. Furthermore, **Rβ** H-2 at δ 3.273 corresponds with the value of a -(1→6)-D-Glc*p* unit and not with that of a -(1→3)-D-Glc*p* unit.[11] The signal at δ 3.42 (dd), shown to correspond to H-4 of a terminal unit, has a surface area of 1H, indicating a linear structure for fraction **5b**. Furthermore, the peak at δ 4.20, outside the bulk-region, has a surface area corresponding to 2H. This peak, with the characteristic shape of an H-5 signal, was established to indicate the presence of -(1→6)-α-D-Glc*p*-**B**-(1→3)- units (see **3b** and **4**). This indicates that both residues **B** are 6-substituted, that is, **X**1→6**B**1→3**Y**. In view of the latter conclusion, the single non-reducing terminal unit **D** must have an α-D-Glc*p*-(1→6)- character. The slight downfield shifts of **Rα** H-1 and **Rβ** H-1 compared to all **R** H-1 signals of isomalto-oligosaccharides,

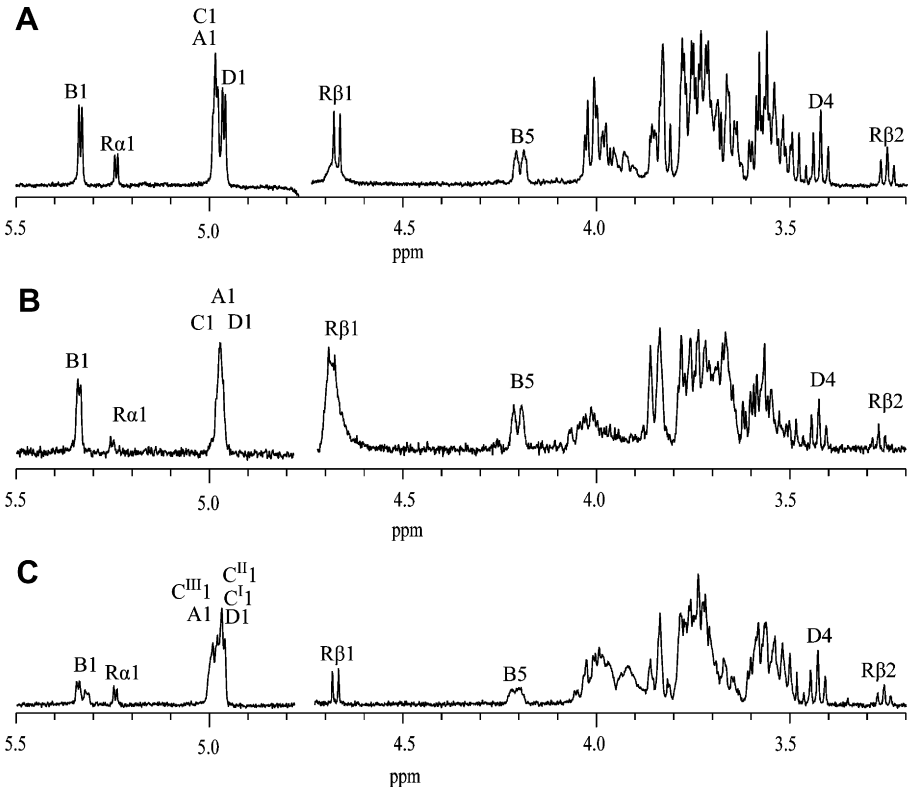

Figure 4. 500-MHz 1D ^{1}H NMR spectra of (A) fraction **4**, (B) fraction **5b** and (C) fraction **8a**, recorded at 300 K in D_2O.

suggest, like in **3b**, a **B**1→3**A**1→6**R** element. In case of the occurrence of a **B**1→3**A**1→6**R** element a splitting of **B** H-1, due to the influence of the α/β configuration of residue **R**, is expected. However, the low signal-to-noise ratio of the NMR spectrum as well as the overlapping of two **B** H-1 signals may interfere with the observation of the expected splitting pattern.

These data lead to two possible structures for **5b**: **D**1→6**C**1→6**B**1→3**A**1→6**B**1→3**A**1→6**R**, that is, α-D-Glc*p*-(1→6)-α-D-Glc*p*-(1→6)-α-D-Glc*p*-(1→3)-α-D-Glc*p*-(1→6)-α-D-Glc*p*-(1→3)-α-D-Glc*p*-(1→6)-D-Glc*p*, or **D**1→6**B**1→3**A**1→6**C**1→6**B**1→3**A**1→6**R**, that is, α-D-Glc*p*-(1→6)-α-D-Glc*p*-(1→3)-α-D-Glc*p*-(1→6)-α-D-Glc*p*-(1→6)-α-D-Glc*p*-(1→3)-α-D-Glc*p*-(1→6)-D-Glc*p* (Scheme 1). The available data do not make a distinction possible.

2.2.6. Fraction 6. The MALDI-TOF-MS analysis of fraction **6** revealed an $[M+Na]^+$ pseudomolecular ion at *m*/*z* 1175, corresponding with Hex_7. HPAEC-PAD analysis on CarboPac PA-1 (eluent: 100 mM NaOAc in 100 mM NaOH) showed one peak. Inspection of the 1D ^{1}H NMR spectrum (not shown) showed a multiple anomeric signal at $\delta \sim 4.96$ (6H; (-)α-D-Glc*p*-(1→6)-), reducing residue anomeric signals at δ 5.240 (**Rα** H-1) and 4.668 (**Rβ** H-1), reflecting the presence of a -(1→6)-D-Glc*p* unit,[11] and a signal at δ 3.42 (dd, 1H), established as a structural reporter for terminal α-D-Glc*p*-(1→*x*)- units.[11] These data identify **6** as isomaltoheptaose, that is, α-D-Glc*p*-(1→6)-α-D-Glc*p*-(1→6)-α-D-Glc*p*-(1→6)-α-D-Glc*p*-(1→6)-α-D-Glc*p*-(1→6)-α-D-Glc*p*-(1→6)-D-Glc*p* (Scheme 1).

2.2.7. Fraction 7. The MALDI-TOF mass spectrum of fraction **7** showed $[M+Na]^+$ pseudomolecular ions at *m*/*z* 851, 1013 and 1175, corresponding with Hex_5, Hex_6 and Hex_7, respectively. The Hex_6 pseudomolecular ion was more intense than those of Hex_5 and Hex_7. Fraction **7** was further separated on CarboPac PA-1 (eluent: 100 mM NaOAc in 100 mM NaOH), rendering one major fraction **7a** (Fig. 2C).

MALDI-TOF-MS analysis of fraction **7a** revealed an $[M+Na]^+$ pseudomolecular ion at *m*/*z* 1013, corresponding with Hex_6. The ^{1}H NMR spectrum (Fig. 5) showed seven anomeric signals at δ 5.343/5.319 (**B** H-1, $^3J_{1,2}$ 3.7 Hz), 5.249 (**Rα** H-1, $^3J_{1,2}$ 3.7 Hz), 4.993 (**A** H-1, **C^{II}** H-1, $^3J_{1,2}$ 3.7 Hz), 4.972 (**C^{I}** H-1, **D** H-1, $^3J_{1,2}$ 3.7 Hz) and 4.679 (**Rβ** H-1, $^3J_{1,2}$ 7.8 Hz). The splitting of the **B** H-1 signal is due to the influence of the α/β configuration of the reducing residue **R** (compare with **3b**). The H-1α and H-1β chemical shift values of **R** correspond to a -(1→6)-α-D-Glc*p* unit, in an (-)α-D-Glc*p*-(1→3)-α-D-Glc*p*-(1→6)-D-Glc*p* element (compare with **3b** and **5b**). The peak at δ 3.43, identified as a structural-reporter-group signal for non-reducing terminal residues,[11] has a surface area corresponding to 1H suggesting a linear structure for **7a**.

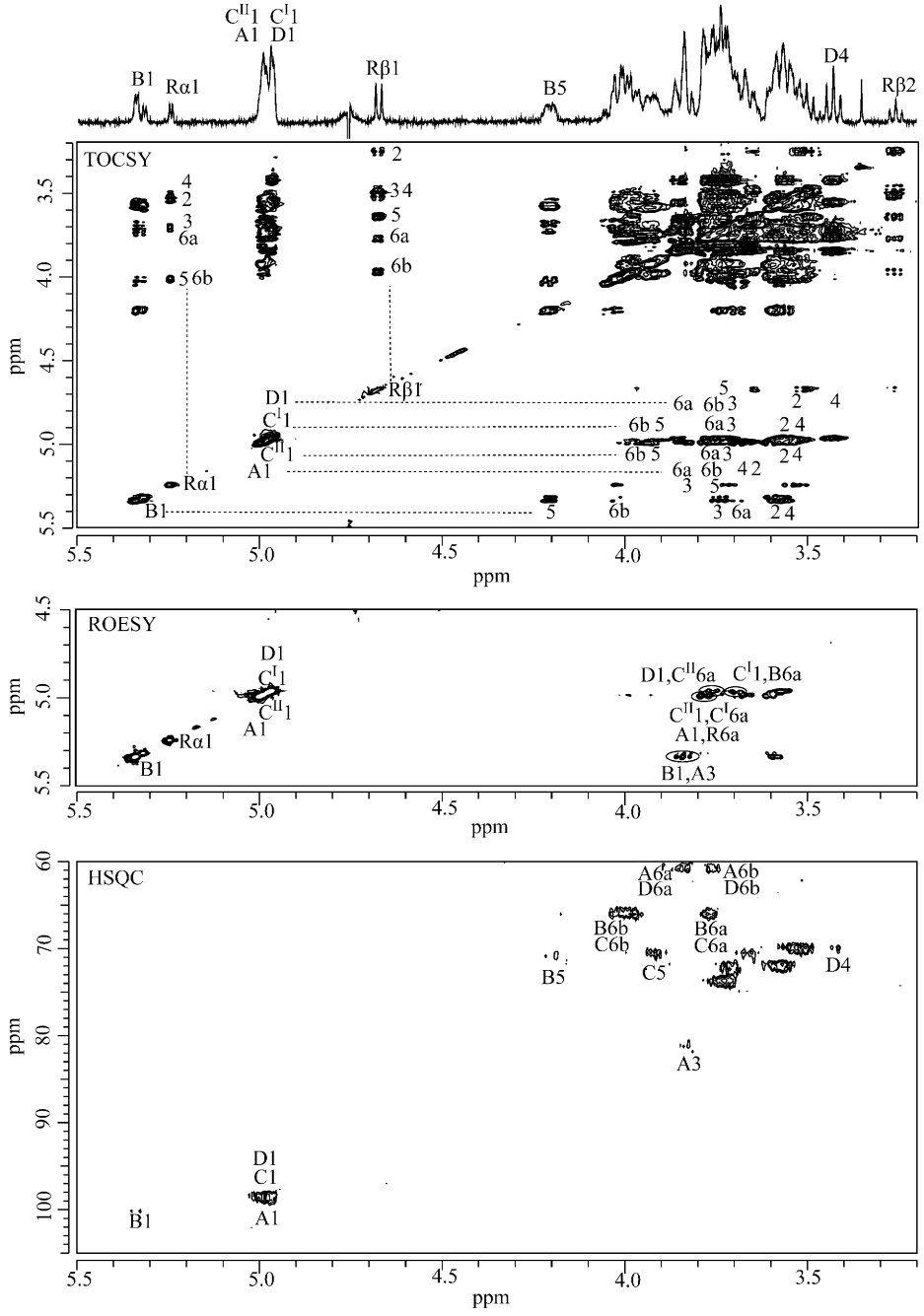

Figure 5. 500-MHz 1D ^{1}H NMR spectrum, 2D ^{1}H–^{1}H TOCSY spectrum (mixing time 180 ms), 2D ^{1}H–^{1}H ROESY spectrum (mixing time 300 ms), and 2D ^{13}C–^{1}H HSQC spectrum of fraction **7a**, recorded at 300 K in D_2O. For an explanation of the coding systems, see Figure 3.

Starting from the anomeric signals in the 2D ^{1}H–^{1}H TOCSY spectrum (Fig. 5), all chemical shifts of the non-anomeric protons were determined (Table 1). The H-1 signals of **A** and **C^{II}**, and of **C^{I}** and **D** overlapped, making it difficult to distinguish between the two residues in each TOCSY track. However, observing the built-up of the scalar coupling network in experiments with increasing mixing times (data not shown), the chemical shifts of each residue could be assigned. On the **A** H-1 track, the set of H-2, H-3 and H-4 is observed at δ 3.64, 3.85 and 3.66, respectively, corresponding with a -(1→3)-α-D-Glc*p*(-) unit, in this case a -(1→3)-α-D-Glc*p*-(1→6)- unit.[11] Residue **C^{II}**, in the same track, showed the proton pattern of a -(1→6)-α-D-Glc*p*-(1→6)- unit, with H-5, H-6a and H-6b at δ 3.94, 3.77 and 3.98, respectively. The **D** H-1 track revealed the chemical shift pattern of a terminal residue, with the most noticeable structural-reporter-group signal H-4 at δ 3.43.[11] Residue **C^{I}**, in the same track, showed a proton pattern similar to **C^{II}**.

The chemical shift of **B** H-5 at δ 4.21 was established as a structural-reporter-group signal for a -(1→6)-α-D-Glc*p*-(1→3)- unit (see **3b**). This is further supported by the chemical shift positions of H-6a (δ 3.70) and H-6b (δ 4.01).[11] The finding that **7a** is a linear structure (see above), having an internal **X**1→6**B**1→3**Y** element, leads to the conclusion that **7a** is built-up of two isomalto-oligosaccharides, interconnected by an (α1→3) linkage. In view of the **B** H-1 splitting, as well as the specific chemical shift values of **R** H-1α and H-1β, indicating a **B**1→3**A**1→6**R** element (see **3b** and **5b**), a **D**1→6$\mathbf{C^{II}}$1→6$\mathbf{C^{I}}$1→6**B**1→3**A**1→6**R** sequence is indicated, that is, α-D-Glc*p*-(1→6)-α-D-Glc*p*-(1→6)-α-D-Glc*p*-(1→6)-α-D-Glc*p*-(1→3)-α-D-Glc*p*-(1→6)-D-Glc*p* (Scheme 1).

The established structure was verified by 2D ^{13}C–^{1}H HSQC and ROESY measurements. Interpretation of the HSQC spectrum (Fig. 5) yielded $\delta_{C\text{-}6}$ values of 66.8 ppm for residues **B**, $\mathbf{C^{I}}$, $\mathbf{C^{II}}$ and **R**, and 61.2 ppm for residues **A** and **D**, indicating 6-substituted **B**, $\mathbf{C^{I}}$, $\mathbf{C^{II}}$ and **R** units.[13] The $\delta_{C\text{-}3}$ value of 81.3 ppm for residue **A** reflects the 3-substitution of this residue.[13] In the ROESY spectrum (Fig. 5), inter-residual cross-peaks were observed. On the **B** H-1 track, a cross-peak was found with **A** H-3 at δ 3.85. On the H-1 track of **D** and $\mathbf{C^{I}}$, cross-peaks were observed with $\delta_{H\text{-}6a}$ 3.70 and 3.77, corresponding to **B** H-6a and $\mathbf{C^{II}}$ or **R** H-6a, respectively. On the H-1 track of **A** and $\mathbf{C^{II}}$, cross-peaks were found with $\delta_{H\text{-}6a}$ 3.76, corresponding to $\mathbf{C^{I}}$ or **R** H-6a. These cross-peaks fit with the structure proposed above.

2.2.8. Fraction 8. The MALDI-TOF mass spectrum of fraction **8** revealed $[M+Na]^+$ pseudomolecular ions at *m*/*z* 1013, 1175 and 1337, corresponding with Hex_6, Hex_7 and Hex_8, respectively, with Hex_7 as the major component. Fraction **8** was further separated on CarboPac PA-1 (eluent: 100 mM NaOAc in 100 mM NaOH); major fraction **8a** was isolated (Fig. 2C).

MALDI-TOF-MS analysis of fraction **8a** revealed an $[M+Na]^+$ pseudomolecular ion at *m*/*z* 1175, corresponding with Hex_7. The 1D ^{1}H NMR spectrum (Fig. 4C) showed eight anomeric signals at δ 5.343/5.320 (**B** H-1, $^{3}J_{1,2}$ 4.0 Hz), 5.246 (**Rα** H-1, $^{3}J_{1,2}$ 4.0 Hz), 4.990 (**A** H-1 and $\mathbf{C^{III}}$ H-1, $^{3}J_{1,2}$ 4.0 Hz), 4.968 ($\mathbf{C^{I}}$ H-1, $\mathbf{C^{II}}$ H-1 and **D** H-1, $^{3}J_{1,2}$ 4.0 Hz) and 4.676 (**Rβ** H-1, $^{3}J_{1,2}$ 7.5 Hz). The H-1α and H-1β chemical shifts of reducing residue **R** correspond to a -(1→6)-α-D-Glc*p* unit, matching the values observed in fraction **3b**, **5b** and **7a**, and suggests a **B**1→3**A**1→6**R** element. The splitting of the **B** H-1 signal is due to the influence of the α/β configuration of the reducing residue **R**, similar to the splitting observed in **3b** and **7a**. The peak at δ 3.43, identified as a structural-reporter-group signal for non-reducing terminal residues,[11] has a surface area corresponding to 1H, suggesting a linear structure for **8a**.

Starting from the anomeric signals in the 2D ^{1}H–^{1}H TOCSY spectrum (not shown), all chemical shifts of the non-anomeric protons could be determined (Table 1). Residues $\mathbf{C^{I}}$, $\mathbf{C^{II}}$ and $\mathbf{C^{III}}$ showed the same chemical shift pattern, with H-5, H-6a and H-6b at δ 3.93, 3.76 and 3.98, respectively. These values were shown to indicate a -(1→6)-α-D-Glc*p*-(1→6)- residue. Residue **B** shows the chemical shift pattern of a -(1→6)-α-D-Glc*p*-(1→3)- unit, with H-5 at δ 4.20 as the most obvious structural-reporter-group signal (see **3b**, **4**, etc.). Residue **B** H-6a and H-6b at δ 3.70 and 4.01, respectively, confirm this observation. Residue **D** shows the chemical shift pattern of a non-reducing terminal residue, with H-4 at δ 3.43 being the most notable structural-reporter-group signal. Taking together all data, this results in a total sequence for compound **8a** of **D**1→6$\mathbf{C^{III}}$1→6$\mathbf{C^{II}}$1→6$\mathbf{C^{I}}$1→6**B**1→3**A**1→6**R**, that is, α-D-Glc*p*-(1→6)-α-D-Glc*p*-(1→6)-α-D-Glc*p*-(1→6)-α-D-Glc*p*-(1→6)-α-D-Glc*p*-(1→3)-α-D-Glc*p*-(1→6)-D-Glc*p* (Scheme 1).

The established structure was verified by 2D ^{13}C–^{1}H HSQC and ROESY measurements. In the HSQC spectrum (not shown), the $\delta_{C\text{-}6}$ values of residues **B**, $\mathbf{C^{III,II,I}}$ and **R** at 66.8 ppm reflect the 6-substitution of these units. The $\delta_{C\text{-}6}$ values of residues **A** and **D** were determined at 61.2 ppm. The $\delta_{C\text{-}3}$ value of 81.2 ppm of residue **A** indicated a 3-substituted residue **A**.[13] In the ROESY spectrum (not shown), inter-residual cross-peaks were observed. Residue **B** H-1 showed one inter-residual cross-peak with **A** H-3. On the **D**, $\mathbf{C^{I,II}}$ H-1 track cross-peaks were observed with $\delta_{H\text{-}6a}$ 3.70 and 3.76–3.77. On the **A**, $\mathbf{C^{III}}$ H-1 track, one inter-residual cross-peak was observed at $\delta_{H\text{-}6a}$ 3.77. These data fit with the proposed sequence for **8a**.

2.3. Smith degradation

To investigate the degree of polymerisation of (α1→3) glycosidic bonds, **EPS180** was subjected to a Smith degradation, comprising of a periodate oxidation, followed by reduction with $NaBH_4$, and mild acid hydrolysis with formic acid. The formed products were analysed by GLC–EI-MS (after trimethylsilylation) and HPAEC-PAD. In view of the linkage analysis (see Section 2.1), α-D-Glc*p*-(1→1)-Gro and [α-D-Glc*p*-(1→3)-]$_n$α-D-Glc*p*-(1→1)-Gro, but also, due to overhydrolysis, Gro, D-Glc and [α-D-Glc*p*-(1→3)-]$_n$D-Glc can be expected.

GLC–EI-MS analysis of the trimethylsilylated residue showed three major products, namely, Gro, D-Glc*p* and α-D-Glc*p*-(1→1)-Gro. Typical fragments for the latter compound comprise *m*/*z* 451 (aA_1), 361 (aA_2), 271 (aA_3), 217 and 204 for the Glc part, and *m*/*z* 219 (bA_1) and 337 (abJ_1) for the Gro part.[14–17]

HPAEC analysis on CarboPac PA-100 of the residue revealed two major peaks that could be related to Gro (t_R 2.3 min) and α-D-Glc*p*-(1→1)-Gro (t_R 6.2 min), which was identified by its elution position, being

slightly later than D-Glc*p* (t_R 5.5 min). Since α-D-Glc*p*-(1→3)-D-Glc*p* under the same conditions has an t_R value >10 min, the presence of [α-D-Glc*p*-(1→3)-]$_n$α-D-Glc*p*-(1→1)-Gro with $n = 1$ or higher could be excluded.

The absence of larger structures than glucosyl-glycerol indicates that the **EPS180** structure does not contain two or more consecutive (α1→3) linkages, but is built-up from isomalto-oligosaccharides, interconnected by single (α1→3) linkages.

2.4. 2D NMR spectroscopy of EPS180

For the unravelling of the 1D ^{1}H NMR spectrum of **EPS180** (Fig. 1B), 2D TOCSY experiments with mixing times of 10, 30, 60, 120 and 180 ms, as well as data from the ^{13}C–^{1}H HSQC measurements of **EPS180** (Fig. 6, Table 1) were interpreted using the data gathered from the oligosaccharides obtained by partial acid hydrolysis of **EPS180** (Section 2.2).

In the 60 ms TOCSY spectrum (330 K, Fig. 6), the H-1 track of residue **B** showed only H-2 and H-3 at δ 3.59 and 3.75, respectively. In the 120 ms TOCSY spectrum (330 K, Fig. 6), the complete scalar coupling network is detected with H-5 at δ 4.17, corresponding with the value found for -(1→6)-α-D-Glc*p*-(1→3)- units (see residue **B** in **3b**, **4**, **5b**, **7a** and **8a**). As the surface area of the H-5 peak at δ 4.17 in the 1D ^{1}H NMR spectrum recorded at 330 K (Fig. 1B) is influenced by the

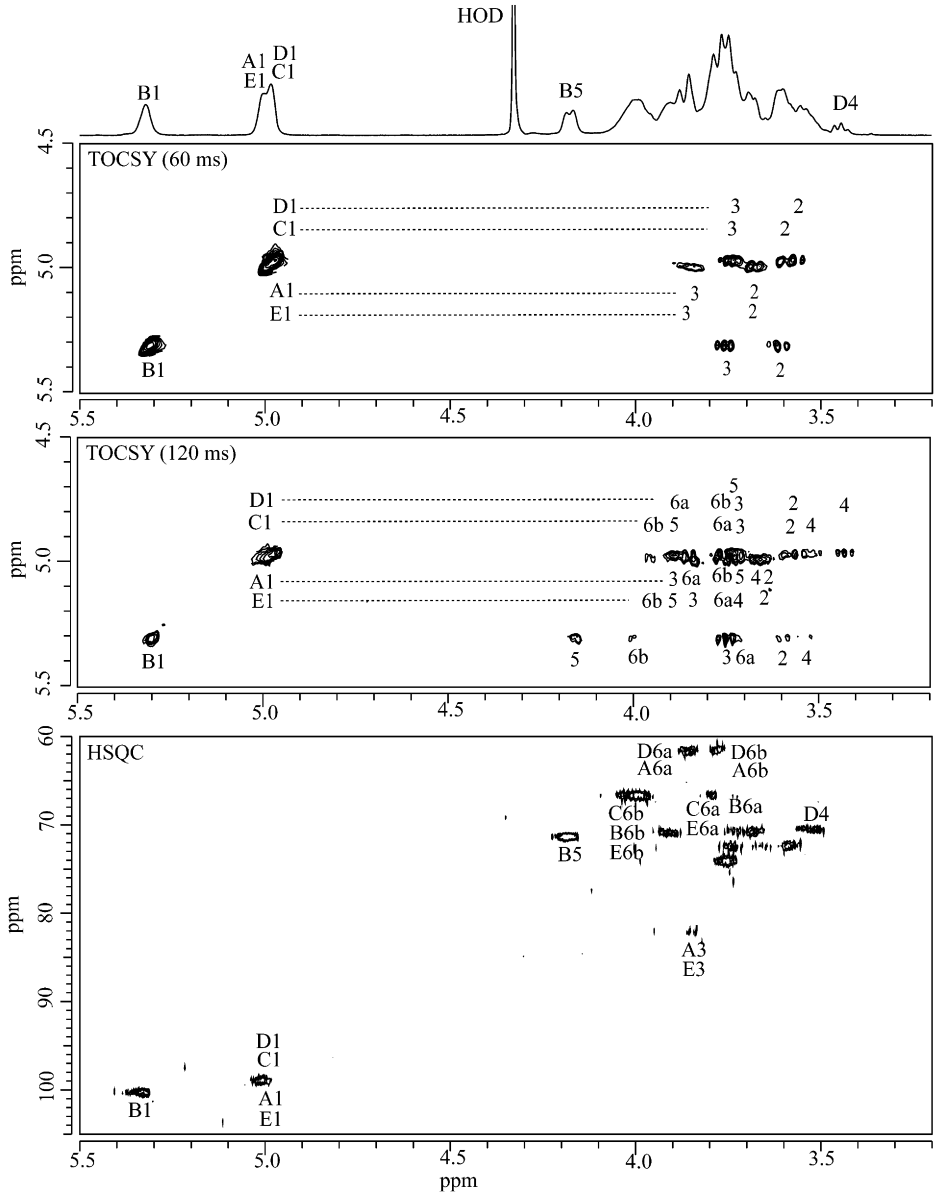

Figure 6. 500-MHz 1D ^{1}H NMR spectrum, 2D ^{1}H–^{1}H TOCSY spectra (top, mixing time 60 ms; bottom, 120 ms) and 2D ^{13}C–^{1}H HSQC spectrum of **EPS180** recorded at 330 K in D_2O. Anomeric protons in the TOCSY spectrum (A1, etc.) have been indicated on the diagonal; numbers in the horizontal tracks belong to the cross-peaks of the scalar-coupling network of the residues indicated. In the ^{13}C–^{1}H HSQC spectrum, A1 denotes the cross-peak between H-1 and C-1 of residue **A**, etc.

suppression of the HOD peak, this signal cannot be used to quantify the occurrence of -(1→6)-α-D-Glc*p*-(1→3)- units in **EPS180**. Fortunately, the 1D ^{1}H NMR spectrum recorded at 300 K (Fig. 1A) can be used for this goal; here, the H-5 signal at δ 4.20 has a surface area matching that of the anomeric peak at δ 5.32, corresponding with (-)α-D-Glc*p*-(1→3)- units. This finding leads to the conclusion that all (-)α-D-Glc*p*-(1→3)- residues are 6-substituted, which is further supported by the absence of an H-4 signal at $\delta \sim 3.43$ (structural-reporter-group signal for terminal residues) and the presence of an H-4 signal at δ 3.52 on the **B** H-1 track (-(1→6)-α-D-Glc*p*(-)).[11] Further support for the conclusion that all (α1→3)-linked residues occur in a -(1→6)-α-D-Glc*p*-(1→3)- element (residue **B**), stems from the absence of cross-peaks in the δ 3.78–3.90 region, typical for H-3 of a 3-substituted residue (nigerotriose),[11] as well as H-6a of a non-6-substituted residue.[11]

The **A**/**E** H-1 track in the 60 ms TOCSY spectrum showed H-2 and H-3 at δ 3.65 and 3.86–3.87, respectively, corresponding to a -(1→3)-α-D-Glc*p*-(1→6)- unit (see residue **A** in **3b**, **4**, **7a** and **8a**). However, the **A**/**E** H-1 track in the 120 ms TOCSY spectrum showed two different H-5 signals at δ 3.70 and 3.90, respectively. The H-5 resonance at δ 3.70 corresponds with the value expected for an (-)α-D-Glc*p*-(1→6)- residue that is not 6-substituted (see residue **A** in **3b**, **4**, **7a** and **8a**),[11] in this case a -(1→3)-α-D-Glc*p*-(1→6)- unit (residue **A**). The H-5 signal at δ 3.90 corresponds with a -(1→6)-α-D-Glc*p*-(1→6)- element (see residue **C** in **4**, **7a** and **8a**, for example). Combined with the H-2 and H-3 δ values that reflect a 3-substitution, this means that a branching -(1→3,6)-α-D-Glc*p*-(1→6)- unit is indicated (residue **E**).

The H-1 track labelled **C**/**D** in the 60 ms TOCSY spectrum showed two overlapping peaks for H-2 at δ 3.57 and 3.55, corresponding with residue types **C** and **D**, respectively (compare with **3b**, **4**, **7a** and **8a**). The **C**/**D** H-1 track revealed one H-3 signal at δ 3.76. These δ values indicate that there is no 3-substitution on these residues (library data: $\delta_{H\text{-}2}$ 3.63–3.68 and $\delta_{H\text{-}3}$ 3.84–3.90 in nigerose and nigerotriose).[11] In the 120 ms TOCSY spectrum, the **C**/**D** H-1 track showed two distinctly different H-4 resonances at δ 3.41 and 3.51. The H-4 signal at δ 3.41 reflects a terminal residue (**D**) and that at δ 3.51 a non-terminal, 6-substituted residue.[11] These chemical shifts allow the distinction between -(1→6)-α-D-Glc*p*-(1→6)- (residue **C**) and α-D-Glc*p*-(1→6)- (residue **D**). In the 120 ms TOCSY spectrum, the **C**/**D** H-1 track showed also peaks for H-5 and H-6b that are shifted downfield, in favour of the 6-substitution of residue **C**.

The substitution patterns established from the TOCSY spectra were verified using ^{13}C–^{1}H HSQC spectroscopy (330 K, Fig. 6). Residues **B**, **C** and **E** gave rise to a $\delta_{C\text{-}6}$ value of 65.9 ppm, reflecting the 6-substitution of these residues.[13] The $\delta_{C\text{-}6}$ value of 61.2 ppm confirmed the absence of a 6-substitution in residues **A** and **D**.[13] Finally, the $\delta_{C\text{-}3}$ value of 81.3 ppm of residues **A** and **E** indicated a 3-substitution.[13]

3. Conclusions

In order to formulate a composite model of the native **EPS180** α-D-glucan, as depicted in Scheme 2, ^{1}H NMR data of **EPS180** were combined with methylation analysis data (Section 2.1) and periodate oxidation data (Section 2.3) of **EPS180**, and with ^{1}H NMR data of the **EPS180** fragments described in Section 2.2. The methylation analysis data together with the ^{1}H NMR data of **EPS180** define the abundances of the five residue types that are the building blocks of the polysaccharide (Table 2). The partial acid hydrolysis fragments (Scheme 1) all fit into the picture, and reflect the structural possibilities within the determined boundaries. It can be concluded that the (1→3,1→6)-α-D-glucan of *L. reuteri* strain 180 has a heterogeneous structure with no repeating units present. It contains only α-D-Glc*p*-(1→6)- units in terminal position. All -α-D-Glc*p*-(1→3)- units were shown to be 6-substituted, and the polysaccharide is built-up from different lengths of isomalto-oligosaccharides, interconnected by single (α1→3) bridges. It should be noted that the advantage of constructing composite models is that α-D-glucans isolated from different bacterial sources or prepared from sucrose by mutant glucansucrases can easily be compared.

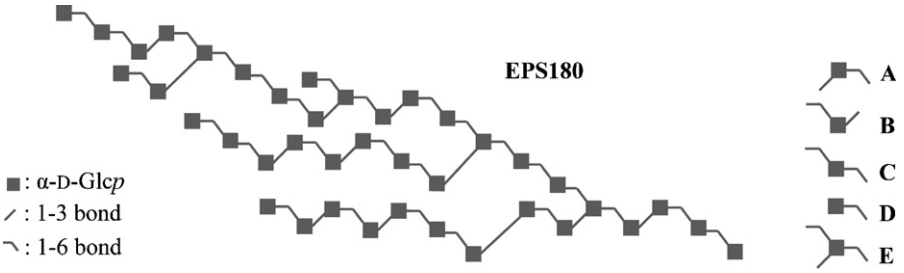

Scheme 2. Composite model of the native **EPS180** α-D-glucan. The composite takes into account all facts from the methylation analysis of **EPS180**, the periodate oxidation study of **EPS180**, and the various ^{1}H NMR analyses of **EPS180** and its established fragments. Residue labels correspond with those used in the text, tables and figures, and are presented on the right.

Table 2. Percentages of building blocks **A**–**E** present in **EPS180**

Building block	Code	Abundance (%)
-(1→3)-α-D-Glc*p*-(1→6)-	**A**	19
-(1→6)-α-D-Glc*p*-(1→3)-	**B**	31
-(1→6)-α-D-Glc*p*-(1→6)-	**C**	26
α-D-Glc*p*-(1→6)-	**D**	12
-(1→3,6)-α-D-Glc*p*-(1→6)-	**E**	12

4. Materials and methods

4.1. Materials

EPS180 was a gift from TNO Quality of Life, Zeist, The Netherlands. D_2O (99.9 atom%) was purchased from Cambridge isotope laboratories, Inc., Andover, MA.

4.2. Monosaccharide analysis

A polysaccharide sample was subjected to methanolysis (1.0 M methanolic HCl, 24 h, 85 °C), followed by re-N-acetylation and trimethylsilylation (1:1:5 hexamethyldisilazane–trimethylchlorosilane–pyridine; 30 min, room temperature). The mixture of trimethylsilylated methyl glycosides was analysed by GLC on an EC-1 column (30 m × 0.32 mm, Alltech Associates Inc., Illinois, USA) using a Chrompack CP 9002 gas chromatograph (temperature gradient, 140–240 °C at 4 °C/min). The identification of the monosaccharide derivatives was confirmed by GLC–EI-MS.[15]

4.3. Linkage analysis

A polysaccharide sample was permethylated using CH_3I and solid NaOH in DMSO, as described earlier.[18] After hydrolysis with 2 M TFA (2 h, 120 °C), the partially methylated monosaccharides were reduced with $NaBD_4$ (2 h, room temperature). Conventional work-up, involving neutralisation with HOAc and removal of boric acid by co-evaporation with MeOH, followed by acetylation with 1:1 acetic anhydride–pyridine (3 h, 120 °C), yielded a mixture of partially methylated alditol acetates, which was analysed by GLC–EI-MS.[15,19]

4.4. Partial acid hydrolysis

In pilot experiments, 5-mg aliquots of **EPS180** were hydrolysed for 30, 60, 90 and 120 min (0.5 M TFA, 90 °C). After concentration under reduced pressure, the residues were analysed by MALDI-TOF-MS and 1D ^{1}H NMR spectroscopy. Based on the initial results, **EPS180** (500 mg) was hydrolysed in 25 mL 0.5 M TFA for 3 h at 90 °C. The solution was concentrated under reduced pressure at a rotary evaporator, and the residue was separated on a Bio-Gel P-4 column (400 × 12 mm, BioRad), eluted with 25 mM NH_4HCO_3; 0.9-mL fractions were collected at a flow rate of 13.5 mL/h. Fractions were tested for the presence of carbohydrate by a TLC spot-test with orcinol/H_2SO_4 staining. Carbohydrate-containing fractions were analysed by MALDI-TOF-MS.

4.5. Smith degradation

EPS180 (50 mg) was incubated with 10 mL 50 mM sodium periodate in 0.1 M NaOAc (pH 4.3) for 96 h at 4 °C in the dark. Then, the excess of periodate was destroyed by the addition of 0.5 mL ethylene glycol. The oxidised polysaccharide solution was dialysed against tap water (24 h, room temperature), treated with excess $NaBH_4$ (18 h, room temperature) and subsequently neutralised with 4 M HOAc.[20] After co-evaporation of boric acid with MeOH, the residue was hydrolysed with 90% HCOOH (30 min, 90 °C). Finally, the solution was concentrated under a stream of N_2, and the products were analysed by GLC–EI-MS and HPAEC-PAD.

4.6. HPAEC-PAD

High-pH anion-exchange chromatography was performed on a Dionex DX500 workstation, equipped with an ED40 pulsed amperometric detection (PAD) system. A triple-pulse amperometric waveform (E_1 0.1 V, E_2 0.7 V, E_3 −0.1 V) was used for detection with the gold electrode.[21] Analytical separations were performed on a CarboPac PA-100 column (250 × 4 mm, Dionex), using a linear gradient of 0–300 mM NaOAc in 100 mM NaOH (1 mL/min). Samples were fractionated on a CarboPac PA-1 column (250 × 9 mm, Dionex), using a linear gradient of 0–300 mM NaOAc in 100 mM NaOH (4 mL/min) or isocratic conditions of 100 mM NaOAc in 100 mM NaOH (4 mL/min). Collected fractions were immediately neutralised with 4 M HOAc, desalted on CarboGraph SPE columns (150 mg graphitised carbon, Alltech) using 1:3 acetonitrile–H_2O as eluent, and lyophilised.

4.7. Mass spectrometry

GLC–EI-MS was performed on a Fisons Instruments GC 8060/ MD 800 system (Interscience BV; Breda, The Netherlands) equipped with an AT-1 column (30 m × 0.25 mm, Alltech), using a temperature gradient of 140–240 °C at 4 °C/min.[15]

Matrix-assisted laser desorption ionisation time-of-flight mass spectrometry (MALDI-TOF-MS) was carried out on a Voyager-DE Pro (Applied Biosystems; Nieuwerkerk aan de IJssel, The Netherlands) instrument in the reflector mode at an accelerating voltage of 24 kV, using an extraction delay of 90 ns, in a resolution of 5000–9000 FWMH. Samples (1 μL) were mixed in a

1:1 ratio with a mixture of 7.5 mg/mL 2,5-dihydroxybenzoic acid (DHB) in 1:1 acetonitrile–H_2O, and spectra were recorded in the positive-ion mode.

4.8. NMR spectroscopy

^{1}H NMR spectra, including ^{1}H–^{1}H and ^{13}C–^{1}H correlation spectra, were recorded on a Bruker DRX500 spectrometer (Bijvoet Center, Department of NMR spectroscopy, Utrecht University). Oligosaccharide ^{1}H NMR spectra were recorded at a probe temperature of 300 K, and intact **EPS180** ^{1}H NMR spectra were recorded at both 300 K and 330 K. Samples were exchanged once with 99.9 atom % D_2O, lyophilised and dissolved in 650 μL D_2O. ^{1}H chemical shifts (δ) are expressed in ppm by reference to internal acetone (δ 2.225), and ^{13}C chemical shifts (δ) are expressed in ppm by reference to the methyl-carbon of internal acetone (δ 31.08). 1D ^{1}H NMR spectra were recorded with a spectral width of 5000 Hz in 16k complex data sets and zero filled to 32k. A WEFT pulse sequence was applied to suppress the HOD signal.[22] When necessary, a fifth order polynomial baseline correction was applied. 2D TOCSY spectra were recorded using MLEV17 mixing sequences with spin-lock times of 10, 30, 60, 120 and 180 ms. The spin-lock field strength corresponded to a 90° pulse width of about 28 μs at 13 dB. The spectral width in 2D TOCSY experiments was 4006 Hz at 500 MHz in each dimension. 400–1024 spectra of 2k data points with 8–32 scans per t_1 increment were recorded. 2D rotating-frame nuclear Overhauser enhancement spectra (ROESY) were recorded with 300 ms mixing time. The spectral width was 4006 Hz at 500 MHz in each dimension. Suppression of the HOD signal was performed by 1 s pre-saturation during the relaxation delay. Between 400 and 1024 data sets of 2k data points were recorded with 8–16 scans per t_1 increment. 2D ^{13}C–^{1}H HSQC spectroscopy was carried out at a ^{1}H frequency of 500.0821 MHz and a ^{13}C frequency of 125.7552 MHz. Spectra were recorded with a spectral width of 4006 Hz for t_2 and 10 kHz for t_1. The HOD signal was pre-saturated for 1 s, and ^{12}C-bound protons were suppressed using a TANGO pulse sequence. During acquisition of the ^{1}H FID, a ^{13}C decoupling pulse was applied. 128–256 experiments of 2k data points were recorded with 128 scans per t_1 increment. 2D NMR spectroscopic data were analysed by applying a sinus multiplication window and zero filling to the spectra of 4k by 1k dimensions. In the case of ^{13}C–^{1}H HSQC data, the spectra were zero filled to 4k by 512 data points. A Fourier transform was applied, and where necessary, a fifth to fifteenth order polynomial baseline function was applied. All NMR data were processed using in-house developed software (J.A. van Kuik, Bijvoet Center, Department of Bio-Organic Chemistry, Utrecht University).

Acknowledgement

This work was financially supported by the Dutch Ministry of Economic Affairs (Senter Novem; Bioprimer project EETK01129).

References

1. Costerton, J. W.; Cheng, K.-J.; Geesey, G. G.; Ladd, T. I.; Nickel, J. C.; Dasgupta, M.; Marrie, T. J. *Annu. Rev. Microbiol.* **1987**, *41*, 435–464.
2. Ceri, H.; McArthur, H. A. I.; Whitfield, C. *Infect. Immun.* **1986**, *51*, 1–5.
3. Cerning, J. *FEMS Microbiol. Rev.* **1990**, *87*, 113–130.
4. Sandford, P. A.; Baird, J. In *The Polysaccharides*; Aspinall, G. O., Ed.; Academic Press: New York, 1983; Vol. 2, pp 411–490.
5. De Vuyst, L.; Degeest, B. *FEMS Microbiol. Rev.* **1999**, *23*, 153–177.
6. Monchois, V.; Willemot, R.-M.; Monsan, P. *FEMS Microbiol. Rev.* **1999**, *23*, 131–151.
7. Funane, K.; Ishii, T.; Matsushita, M.; Hori, K.; Mizuno, K.; Takahara, H.; Kitamura, Y.; Kobayashi, M. *Carbohydr. Res.* **2001**, *334*, 19–25.
8. Argüello-Morales, M. A.; Remaud-Simeon, M.; Pizzut, S.; Sarçabal, P.; Willemot, R.-M.; Monsan, P. *FEMS Microbiol. Lett.* **2000**, *182*, 81–85.
9. Kralj, S.; van Geel-Schutten, G. H.; van der Maarel, M. J. E. C.; Dijkhuizen, L. *Microbiology* **2004**, *150*, 2099–2112.
10. Gibson, G. R.; Roberfroid, M. B. *J. Nutr.* **1995**, *125*, 1401–1412.
11. Van Leeuwen, S. S.; Leeflang, B. R.; Gerwig, G. J.; Kamerling, J. P. *Carbohydr. Res.* **2008**, doi:10.1016/j.carres.2008.01.043.
12. Dowd, M. K.; Zeng, J.; French, A. D.; Reilly, P. J. *Carbohydr. Res.* **1992**, *230*, 223–244.
13. Bock, K.; Thøgersen, H. *Ann. Rep. NMR Spectrosc.* **1982**, *13*, 2–57.
14. Kovacik, V.; Bauer, S.; Rosik, J.; Kovac, P. *Carbohydr. Res.* **1968**, *8*, 282–290.
15. Kamerling, J. P.; Vliegenthart, J. F. G. In *Mass Spectrometry*; Lawson, A. M., Ed.; Clinical Biochemistry—Principles, Methods, Applications; Walter de Gruyter: Berlin, 1989; Vol. 1, pp 176–263.
16. Van der Kaaden, A.; van Doorn-van Wakeren, J. I. M.; Kamerling, J. P.; Vliegenthart, J. F. G.; Tiesjema, R. H. *Eur. J. Biochem.* **1984**, *141*, 513–519.
17. Veerkamp, J. H.; van Schaik, F. W. *Biochim. Biophys. Acta* **1974**, *348*, 370–387.
18. Ciucanu, I.; Kerek, F. *Carbohydr. Res.* **1984**, *131*, 209–217.
19. Jansson, P.-E.; Kenne, L.; Liedgren, H.; Lindberg, B.; Lönngren, J. *Chem. Commun. Univ. Stockholm* **1976**, *8*, 1–74.
20. Hay, G. W.; Lewis, B. A.; Smith, F. *Methods Carbohydr. Chem.* **1965**, *5*, 357–360.
21. Lee, Y. C. *Anal. Biochem.* **1990**, *189*, 151–162.
22. Hård, K.; van Zadelhoff, G.; Moonen, P.; Kamerling, J. P.; Vliegenthart, J. F. G. *Eur. J. Biochem.* **1992**, *209*, 895–915.